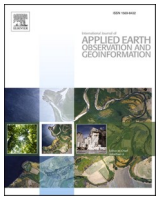
International Journal of Applied Earth Observation and Geoinformation 130 (2024) 103838



Contents lists available at ScienceDirect

International Journal of Applied Earth Observation and Geoinformation

journal homepage: www.elsevier.com/locate/jag



Spatiotemporal monitoring of grasshopper habitats using multi-source data: Combined with landscape and spatial heterogeneity

Jing Guo [a,b], Wenjiang Huang [a,b,*], Yingying Dong [a,b,*], Kejian Lin [c], Yantao Zhou [d,e], Ning Wang [c], Rui Hua [c], Zhuoqing Hao [a,b], Xiaolong Ding [c], Fei Zhao [f]

[a] State Key Laboratory of Remote Sensing Science, Aerospace Information Research Institute, Chinese Academy of Sciences, Beijing 100094, China
[b] University of Chinese Academy of Sciences, Beijing 100049, China
[c] Key Laboratory of Biohazard Monitoring and Green Prevention and Control in Artificial Grassland, Ministry of Agriculture and Rural Affairs, Institute of Grassland Research, Chinese Academy of Agricultural Sciences, Hohhot 010010, Inner Mongolia, China
[d] Center for Biological Disaster Prevention and Control, National Forestry and Grassland Administration, Shenyang 110034, China
[e] Key Laboratory of National Forestry and Grassland Administration on Forest and Grassland Pest Monitoring and Warning, Shenyang 110034, China
[f] School of Earth Sciences, Yunnan University, Kunming 650500, China

ARTICLE INFO

Keywords:
Pest
Remote sensing
Grassland
Spatiotemporal characteristics
Habitat monitoring

ABSTRACT

Grasshoppers, as pernicious pests, pose a formidable threat to the advancement of agriculture and animal husbandry. Their presence can elicit a cascade of environmental challenges, underscoring the pressing need for effective control measures. However, grasshopper development is an intricate process influenced by diverse environmental factors with varying weights across regions, making it difficult to prevent and control. Therefore, this study focused on the prevalent infestation region, Xilingol, and selected *Dasyhippus barbipes* as the research subject because of its highest density and largest damaged area. Initially, according to the development mechanisms of *D. barbipes*, 31 habitat factors from five categories (meteorology, vegetation, soil, topography, and ecology) were selected; then, difference tests, correlation analysis, importance tests, and principal component analysis were applied to construct representative indicators for monitoring the habitat of *D. barbipes* (HDB). Subsequently, employing the occurrence data of *D. barbipes* from 2018 to 2023, a spatial pattern analysis was conducted to explore the hotspot aggregation area (HAA) and spatiotemporal characteristics of *D. barbipes*. Finally, considering landscape and spatial heterogeneity, the Landscape-based Geographically Weighted Logistic Regression (L-GWLR) model for HDB was constructed to achieve adaptive changes in factor weights across regions. The indicators included minimum temperature during the egg stage, precipitation, and soil temperature during the spawning stage, slope, fractional vegetation coverage in the nymph stage, soil moisture in the 1st to 3rd nymph instar, patch area, and gyration radius. The spatial pattern analysis revealed a significant spatial autocorrelation in the distribution of *D. barbipes* at a 90 % confidence interval ($z > 1.65$ and $p < 0.1$), and HAAs were concentrated in West Ujimqin, XilinHot, and ZhengLan. The habitat monitoring results demonstrated the superior performance of the L-GWLR model over models neglecting landscape or spatial heterogeneity. These findings provide essential support for the environmentally friendly scientific control of grasshoppers, contributing significantly to the sustainable development of agriculture and animal husbandry.

1. Introduction

Grasslands are crucial components of terrestrial ecosystems and play vital roles in preserving water sources, protecting biodiversity, and safeguarding food production (Petermann and Buzhdygan, 2021). Grasslands, which include open grasslands, grassy shrublands, and savannas, account for about 40 % of the Earth's surface and 69 % of its agricultural land area (O' Mara, 2012). However, grassland ecosystems

Abbreviations: D^2, Percentage Deviance Explained; GYRATE, Radius of Gyration; HAA, Hotspot aggregation area; L-GWLR, Landscape based Geographically Weighted Logistic Regression; N1SM, Soil moisture of the 1th to 3th nymph instar; Nfvc, FVC in the nymph period; OLS, Ordinary Least Squares regression; OMinT, Minimum temperature in the egg stage; SP, Total precipitation in the spawning period; SST, soil temperature in the spawning period.

* Corresponding authors.
E-mail addresses: huangwj@aircas.ac.cn (W. Huang), dongyy@aircas.ac.cn (Y. Dong).

https://doi.org/10.1016/j.jag.2024.103838
Received 4 February 2024; Received in revised form 31 March 2024; Accepted 13 April 2024
Available online 8 May 2024
1569-8432/© 2024 Published by Elsevier B.V. This is an open access article under the CC BY-NC-ND license (http://creativecommons.org/licenses/by-nc-nd/4.0/).

encounter massive threats from insect pests, leading to considerable damage such as grassland degradation and land desertification. Consequently, grassland degradation and land desertification can exacerbate insect pest proliferation, thereby initiating a destructive cycle. Among the various pests, one of the most formidable threats is grasshoppers, which are widely distributed in grassland regions, affecting a population of up to 850 million people and causing significant impacts (Chen, 2008).

China has suffered from locust plagues over its long history, tracing back to the oracle bone script period. Grasshoppers are prevalent in 13 provinces and autonomous regions in China, including Inner Mongolia, Xinjiang, and Gansu. The annual average grasshopper infestation area in these regions was approximately 40 million hectares. At an average grass yield loss of 450 kg/ha and value of 0.3 yuan/kg (Tu et al., 2015), the direct economic losses caused by grasshoppers in China reach nearly 5 billion yuan annually. One of the most severely affected regions is Xilingol, which has various grasshopper species owing to its rich diversity of grassland types, favorable climatic conditions, and expansive grassland areas. The most damaging grasshoppers in recent years is *Dasyhippus barbipes* (Fischer-Walheim), with densities reaching 167 individuals/m^2. Notably, economic and ecological losses occur when the density exceeds 22.7 individuals/m^2 (Qiu et al., 2004). Therefore, monitoring measures and early warning systems must be developed to minimize losses.

The current monitoring methods for grasshoppers primarily include field surveys and remote sensing. Field surveys can achieve a high accuracy in localized areas. However, China, which has the largest global grassland area, faces challenges in meeting the demand for precise large-scale pest control only using field surveys. Moreover, the ongoing effects of climate change and human activities have led to dynamic shifts in their suitable habitats (Sivakumar et al., 2013; Zhang et al., 2019; Meynard et al., 2020), further complicating grasshopper prevention and control efforts. With the advancement of remote sensing technology, satellites with high spatiotemporal resolution have formed into monitoring networks. Coupled with fundamental geographic, land use/land cover, long-term meteorological reanalysis, and ground-based survey data, a wealth of spatiotemporally continuous and diverse data resources has been provided for the dynamic monitoring of pests. This has enabled large-scale continuous monitoring wherever possible (Waldner et al., 2015; Löw et al., 2016).

However, owing to the small size of grasshoppers, which are approximately a few centimeters in length, existing optical remote sensing technologies struggle to achieve such a fine spatial resolution, making it challenging to directly monitor and identify them from satellite imagery. Consequently, current remote sensing-based locust monitoring studies often focus on acquiring habitat factors closely associated with the developmental stages of locusts, such as vegetation, meteorological conditions, soil characteristics, and topography, and identifying their impact mechanisms on locust growth, development, and reproduction (Latchininsky, 2008; Gómez et al., 2019; Ahmad et al., 2022; Klein et al., 2023). Certain studies have monitored and analyzed the evolution of locust habitat using expert models, machine learning, deep learning, and ecological niche models and have yielded significant positive outcomes (Tappan et al., 1991; Piou et al., 2013; Zhao et al., 2020).

In summary, extensive research has been conducted on the mechanisms of locust occurrence and the influence of habitat factors, as well as on monitoring the habitat of locusts. However, several problems remain unresolved. The grasshoppers exhibit diverse types, and the occurrence and development of each species are influenced by multiple habitat factors. Consequently, the interaction mechanisms between different species of grasshoppers and habitat factors vary. Moreover, the regional characteristics and dominant factors differ among the various regions. Therefore, this study aimed to accomplish the following objectives: 1) establish representative monitoring indicators for *D. barbipes* based on its developmental mechanisms; 2) identify the hotspot aggregation area (HAA) and spatiotemporal characteristics of *D. barbipes*; 3) develop a continuous and dynamic monitoring model for the habitat of *D. barbipes* (HDB), considering landscape and spatial heterogeneity, and analyze the driving factors that influence its spatiotemporal evolution. The results can be developed as methodological support to guide related grasshoppers' precautions and control and are beneficial for ensuring ecological environment security and promoting sustainable husbandry development.

2. Materials and methods

To begin, we applied the degree day model to ascertain the developmental stages of *D.barbipes* based on its development mechanism. Subsequently, we identified environmental factors influencing the growth of *D.barbipes*, including vegetation, meteorology, soil, topography, and landscape. Difference tests, correlation analysis, importance testing, and principal component analysis were utilized to construct the most representative monitoring index. Moreover, we employed global and local spatial autocorrelation analysis methods alongside kernel density analysis to unveil the spatial characteristics of *D.barbipes*. Leveraging these findings and considering both the spatial characteristics of *D.barbipes* and the landscape, we constructed the L-GWLR model to monitor habitat dynamic changes. Finally, we analyzed the driving factors behind these habitat dynamic changes (Fig.1).

2.1. Study area

The study area is located in Xilingol, Inner Mongolia Autonomous Region, China (Fig. 2) (41.57°–46.77°N, 111.14°–119.98°E), and covers two county-level cities, one county, nine banners, and one administrative district spanning a total area of 203,000 km^2 (Lian and Leng, 2007). The grassland area within the region is approximately 191,400 km^2 (Liu, 2020), and encompasses various types, such as typical temperate, temperate meadows, and temperate desert grasslands (Huang et al., 2009; Dong et al., 2022). The expansive grassland area and varied grassland types contribute to the diverse range of grasshopper species in the research area, totaling 59 species spanning the early, mid, and late stages (Guo, 2007). In Xilingol, the grasshopper infestation area reaches up to 16 million mu annually, with the primary damaging species being *D. barbipes* (Fischer-Walheim), *Oedaleus decorus asiaticus* (B.-Bienko), *Paracyptera microptera* (Ikonnikov), and *Angaraciris barabensis* (Pallas) (Shen et al., 2015). Among these, the most numerous and densely populated species (up to 176/m^2) in recent years is the early-stage species *D. barbipes*, which causes severe damage to multiple banners and counties, including West Ujumqin, East Ujumqin, XilinHot, Zheng Lan, Xiang Huang, Zheng Xiang Bai, and Duo Lun. Therefore, this study focuses on the research of *D. barbipes* as the target species.

We divided the study area into four sub-regions. Area 1 encompasses five counties, including Zheng Lan, Xiang Huang, Zheng Xiang Bai, TaiPuSi, and Duo Lun. These counties share similar habitat conditions for grasshoppers. Area 2 includes XilinHot, West Ujumqin, Abaga, Sunit Right, and Sunit Left. Among them XilinHot and West Ujumqin are more susceptible to grasshopper infestations, resulting in the highest level of damage each year. Area 3 primarily consists of East Ujumqin (excluding WuLaGai), while Area 4 refers specifically to WuLaGai within East Ujumqin. Although WuLaGai is geographically part of East Ujumqin, it shares a border with Mongolia and experiences colder weather compared to other farmlands in East Ujumqin. Additionally, the grassland type in WuLaGai differs from that of the surrounding areas. Hence, we delineated it as a separate area within our study.

2.2. Data acquisition and processing

2.2.1. Satellite data

The MOD11A1 and MOD13A2 products of MODIS, spanning the period from 2017 to 2023, were employed to acquire the land surface

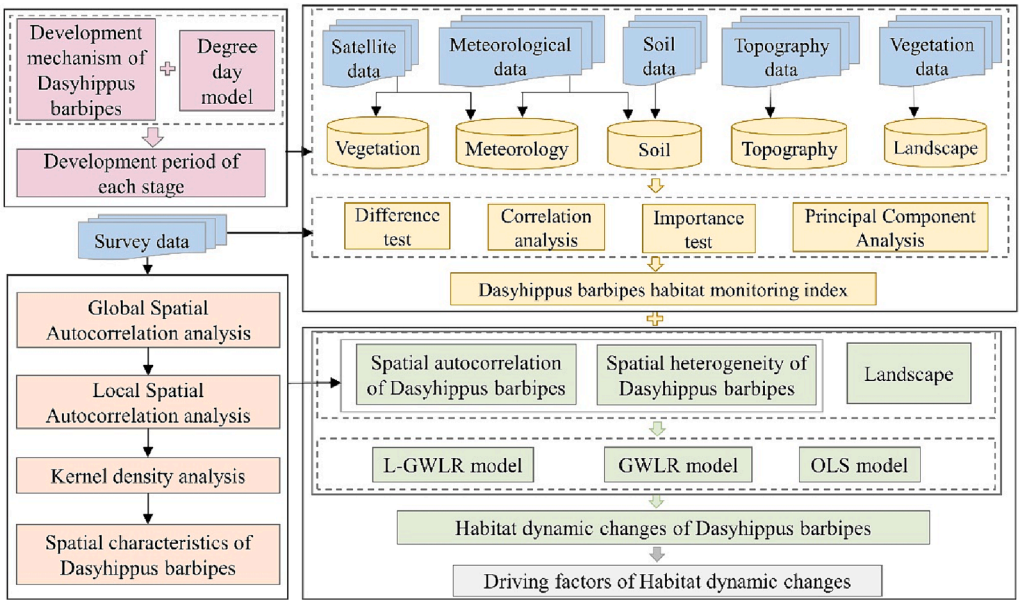


Fig. 1. Flowchart of the paper.

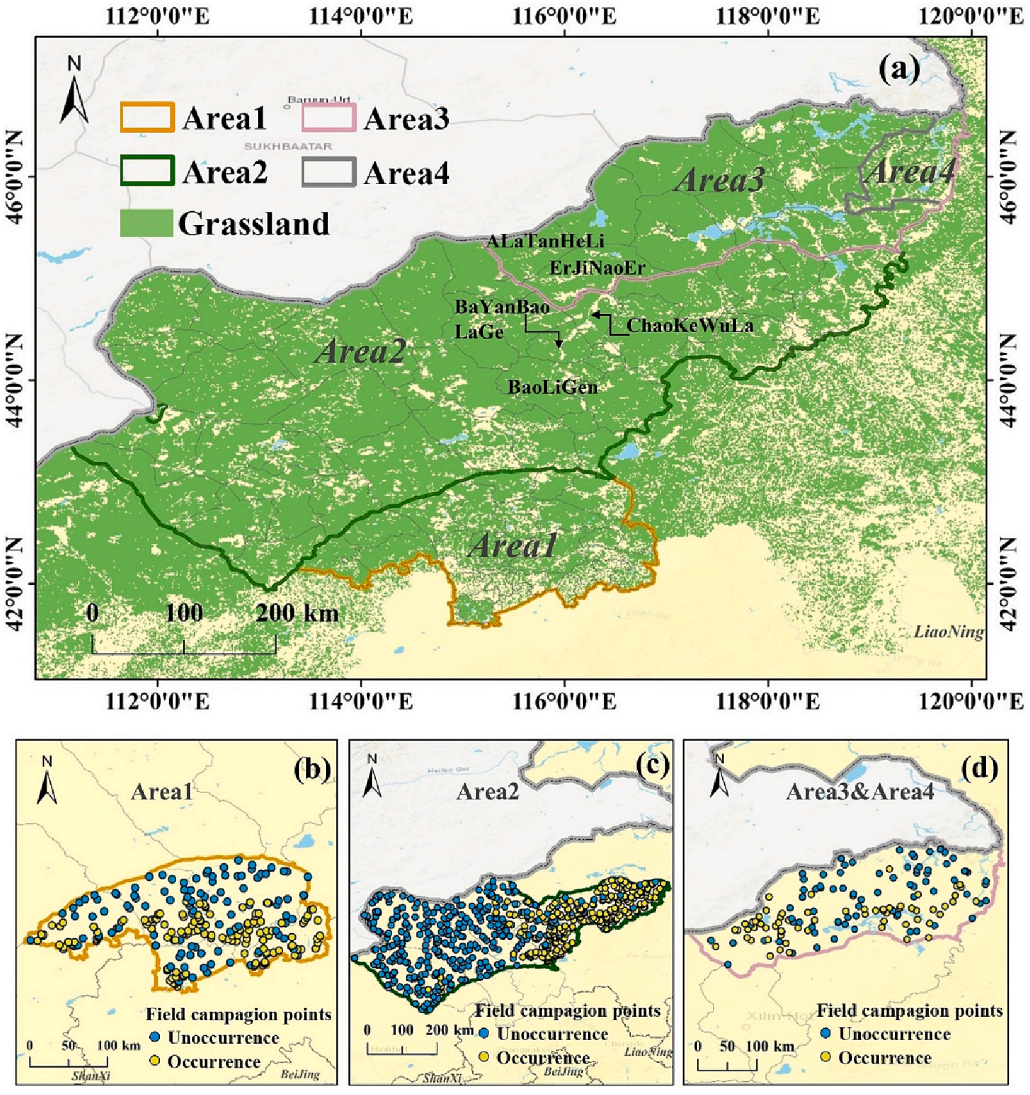


Fig. 2. Location map of the study area.

temperature and normalized difference vegetation index. The land surface temperature data consisted of both mean and minimum temperature with a temporal resolution of 1 day and a spatial resolution of 1 km. Normalized difference vegetation index data were used to compute the Fractional Vegetation Cover (FVC) with a temporal resolution of 16 days and a spatial resolution of 1 km.

2.2.2. Meteorological data

The meteorological data utilized in this study, spanning from 2017 to 2023, consisted of several datasets, which includes the ERA5_LAND dataset (band: soil temperature level 1) (Geng et al., 2020), precipitation data sourced from the European Centre for Medium-Range Weather Forecasts and Global Precipitation Measurement (band: precipitationCal), and Soil Moisture Active Passive data (band: sm_surface). The soil temperature data encompassed mean and minimum soil temperatures. These datasets maintain a spatial resolution of 9 km for soil temperature and moisture, while precipitation data is at a spatial resolution of 10 km. Additionally, the temporal resolution for soil temperature, soil moisture, and precipitation data is 1 h, 3 h, and 3 h, respectively.

2.2.3. Soil and topography data

In general, the soil type, nitrogen, pH, clay type, and topography (ground elevation, aspect, and slope) in the study area remained unchanged. Consequently, this study posits that these conditions remained relatively stable throughout the study period. Soil-type data were sourced from a national database updated in 2015. Soil nitrogen (5–15 cm), pH (5–15 cm), and clay (5–15 cm) data were acquired from Soilgrids 250 m (https://www.soilgrids.org).

All satellite, meteorological, soil, and topographic data were downloaded and calculated using the Google Earth Engine. After preprocessing, which involved mosaicking, masking, and re-projection, all data were resampled to a spatial resolution of 1 km.

2.2.4. Landscape data

The landscape data used in this study were derived from a vegetation-type dataset provided by the Institute of Geographic Sciences and Natural Resources Research, Chinese Academy of Sciences (Du et al., 2022). The study area encompasses 105 vegetation types distributed across 1042 patches.

2.3. Field campaign

The data used in this study were collected through field surveys conducted between 2018 and 2023. Experiments were conducted in accordance with the standards of the agricultural industry of the People's Republic of China (NY/T 1578–2007, rules for investing locality and grasshopper in grassland). The investigation treated each pasture as a basic unit. The minimum average interval for setting up the sampling plots was 10 km. Each sampling plot measured 1 × 1 km to maintain consistency with the spatial resolution of the habitat indicator data. Within each sampling plot, 10 sub-plots with a size of 1 × 1 m were randomly selected to collect the geographical coordinates, grasshoppers' numbers, types, and densities within each plot. Field surveys were undertaken between 09:00–17:00 on sunny days and conducted annually during the nymph and adult periods of *D. barbipes* (May to July) from 2018 to 2023 in the study area. A total of 501 occurrence points and 519 non-occurrence points for *D. barbipes* were obtained (Fig. 2b, 2c, 2d).

2.4. Monitoring indicators

The grasshopper life cycle is divided into three stages: egg, nymph, and adult (Vennard et al., 1998). During each stage, the temperature is the primary factor influencing grasshopper growth and development (Ge et al., 2009). They must reach an initial temperature and accumulate a defined amount of heat to transition to the subsequent stage; otherwise, they enter a state of diapause. Previous studies did not divide the study area into subregions but rather assumed uniformity in the growth and development of grasshoppers within the Xilingol. Moreover, they employed empirical methods to define the developmental stages of grasshoppers. (Guo et al., 2023). However, owing to temperature variations, the developmental time of *D. barbipes* within the research area exhibits some inconsistencies. In the southern and northern regions, the peak hatching period generally occurs in April and May, respectively. Thus, relying on experiential knowledge may introduce inaccuracies in identifying the precise developmental period of *D. barbipes*, which is a crucial prerequisite for habitat factor selection. To more accurately obtain the developmental period of *D. barbipes*, this study, based on the historical occurrence patterns of *D. barbipes* and environmental conditions, divided the research area into four sub-regions. By combining the growth and development mechanisms of *D. barbipes* (Bai, 2012) with the degree day model, we calculated their growth and development in each sub-region. The effective accumulation temperature for *D. barbipes* was obtained from Chen et al. (2008).

Various factors impact the occurrence and development of grasshoppers, including meteorology, soil, vegetation, topography, and ecology (Pegel et al., 2019; Geng et al., 2022; Bernard et al., 2023). The meteorological factors that play a pivotal role include soil temperature, surface temperature, and precipitation. Soil type, pH, and sand content influence their distribution (Edwards and Epp, 1965), and soil moisture is closely related to the hatching rate (Gómez et al., 2020). Vegetation, which is the main habitat and food source for grasshoppers, is important for oviposition, hatching, and growth. Vegetation type influences their feeding preferences, with *O. decorus asiaticus* preferring *Leymus chinensis* (Li et al., 2021), while Asian migratory locusts preferring reeds (Guo et al., 2022). Topographical factors also play a crucial role in grasshopper distribution. Research indicates that grasshoppers are primarily located in regions with elevations of 1400–1500 m (Wachter et al., 1998). Slope determines the distribution and feeding patterns of grasshoppers (Coxwell and Bock, 1995).

Furthermore, landscape play a pivotal role in grasshopper occurrences. Due to the significant influence of vegetation types on grasshopper feeding and habitat suitability, this study regarded vegetation type as a vital factor in examining the impact of landscape characteristics on the distribution of *D. barbipes*. At the patch scale, this study selected eight indicators reflecting landscape area, edge, and shape characteristics (Table S1) and calculated the corresponding landscape indicators using Fragstats 4.2 software (http://www.umass.edu/landeco/research/fragstats/fragstats.html). In summary, this study selected 14 static and 17 dynamic factors (Table S1), covering meteorology, soil, vegetation, topography, and landscape categories across the three life stages of grasshoppers.

To construct the most representative monitoring indicators for HDB, 1020 points over six years were employed for subsequent analysis. First, normal distribution tests were applied to assess the distribution characteristics of each factor, and appropriate differential test methods were selected based on the distribution characteristics. Specifically, t-tests were used for normally distributed factors, Wilcoxon rank-sum tests for non-normally distributed factors, and chi-square tests for categorical variables. Factors with no significant differences in the 95 % confidence interval (p-value > 0.05) were eliminated. To avoid strong correlations between variables, we conducted a Spearman correlation analysis on factors with significant differences. During the variable selection process, the random forest method was employed to assess the importance of the indicators. The factors that displayed correlations exceeding 0.8 and gained lower importance were removed (Xu et al., 2018).

Landscape variables differ from local habitat variables. Therefore, testing methods for local variables may not be applicable. This study adopted correlation analysis and Principal Component Analysis (PCA) to optimize landscape variables. First, a correlation analysis was conducted on landscape factors to explore significant correlations between

variables. In instances where the correlation between two variables exceeded 0.8, the PCA method was used to optimize the variables. Finally, the landscape indicators with the greatest impact on the *D. barbipes* were retained.

2.5. Spatial pattern analysis for D. barbipes

The distribution of grasshoppers in the prairie is not random (Gauffre et al., 2015); instead, it exhibits certain spatial characteristics. Consequently, this study aimed to explore the HAAs and spatiotemporal features of *D. barbipes* to elucidate its spatiotemporal distribution pattern. Based on historical occurrence data from 2018 to 2023, the Global Moran's I index was applied to assess the overall spatial autocorrelation of *D. barbipes*. Within the 90 % confidence interval, a z-score > 1.65 with a p-value < 0.1 indicated significant positive spatial autocorrelation, while a z-score < -1.65 with a p-value < 0.1 showed significant negative spatial autocorrelation.

After analyzing the overall spatial characteristics of *D. barbipes*, a local significance hotspot analysis was conducted using the Getis-Ord General Gi* statistic (Getis and Ord, 1992). This statistic identifies statistically significant hotspots by calculating the value of each geographic element and determining whether the units belong to a particular hotspot. Assuming normal distribution testing at a 5 % confidence interval, hotspots were identified among units with a z-score > 1.96 and a significant p-value < 0.1.

To further explore the HAA and spatiotemporal distribution patterns of *D. barbipes*, the Kernel Density Estimation method was employed by analyzing the significant hotspots. Finally, the Standard Deviation Ellipse (SDE) was employed to reveal the overall spatial distribution and spatiotemporal variation characteristics of *D. barbipes*.

2.6. HDB monitoring model with landscape and spatial heterogeneity

Grasshoppers are influenced not only by local habitat factors but also by landscape factors. Landscape type and number of patches can affect species distribution (Steck et al., 2006). Many studies on grasshoppers focus solely on local factors, this limitation weakens the accuracy of the model (Shi et al., 2018; Geng et al., 2020; Zhao et al., 2020). The landscape factors have contributed to the occurrence of grasshoppers. Furthermore, the impact of multi-source habitat factors on grasshopper occurrence is not constant. The weights of these factors vary across different regions, leading to spatial autocorrelation and heterogeneity in grasshopper occurrence (Humphreys et al., 2022). Hence, models overlooking landscape and spatial variabilities are incomplete.

Building on the aforementioned analysis and the monitoring indicators established in Section 2.4, this study constructed an L-GWLR model for HDB combined with the advantages of Logistic Regression (LR) and Geographically Weighted Logistic Regression (GWR), which considers multi-source factors, landscape, and spatial heterogeneity. The model's expression is shown in Equation (2)–(2): The probability of grasshopper occurrence at the location is denoted as P, and the probability of no grasshopper occurrence at the same location is $(1 - P)$. Therefore, the probability of grasshoppers occurring at the location can be represented as follows:

$$P(Y=1) = \frac{\exp(\alpha_{0(u_i,v_i)} + \alpha_{1(u_i,v_i)}x_{i1} + \alpha_{2(u_i,v_i)}x_{i2} + \ldots + \alpha_{n(u_i,v_i)}x_{in})}{1 + \exp(\alpha_{0(u_i,v_i)} + \alpha_{1(u_i,v_i)}x_{i1} + \alpha_{2(u_i,v_i)}x_{i2} + \ldots + \alpha_{n(u_i,v_i)}x_{in})} = \frac{1}{1 + \alpha_{0(u_i,v_i)} + \alpha_{1(u_i,v_i)}x_{i1} + \alpha_{2(u_i,v_i)}x_{i2} + \ldots + \alpha_{n(u_i,v_i)}x_{in}} \tag{2-2}$$

After applying the Logit transformation, we have

$$\text{Logit(P)} = \ln\frac{P}{1-P} = \alpha_{0(u_i,v_i)} + \alpha_{1(u_i,v_i)}x_{i1} + \alpha_{2(u_i,v_i)}x_{i2} + \ldots + \alpha_{n(u_i,v_i)}x_{in} \tag{2-3}$$

Finally, the parameters of the local regression model for location can be obtained using the weighted least squares method:

$$\widehat{\alpha}_{(u_i,v_i)} = \left(X^T W(u_i,v_i)X\right)^{-1} X^T W(u_i,v_i)\text{log}it(P) \tag{2-4}$$

where (u_i, v_i) are the geographical coordinates of i, $\alpha_{0(u_i,v_i)} + \alpha_{1(u_i,v_i)}x_{i1} + \alpha_{2(u_i,v_i)}x_{i2} + \ldots + \alpha_{n(u_i,v_i)}x_{in}$ is the estimated value, $W(u_i, v_i)$ is the matrix weight, and X represents the matrix of explanatory variables.

To compare the applicability and accuracy of these models, this study employed L-GWLR, GWR, LR, and classical Ordinary Least Squares (OLS) regression model models to explore the optimal monitoring method. Model performance was evaluated using two accuracy metrics: the percentage deviance explained (D^2) and the Akaike Information Criterion (AIC). Higher D^2 values indicate better explanatory effects of the independent variables on the dependent variables, reflecting stronger model interpretability. Lower AIC values indicate better model fitting.

On this basis, regarding the study of monitoring grasshopper habitat in Xilingol (Guo et al., 2023), the monitoring results of *D. barbipes* were classified into three levels based on the probability of occurrence: less suitable ($0 < P \leq 0.5$), moderately suitable ($0.5 < P \leq 0.7$), and most suitable ($0.7 < P \leq 1$). Subsequently, this study analyzed the spatiotemporal evolution changes of HDB and revealed the driving factors behind their spatiotemporal changes.

3. Results

3.1. Construction of monitoring indicators

This study employed the degree day model, coupled with the growth and development mechanisms of *D. barbipes*, to calculate developmental periods in four sub-regions. The results (Fig. 3a) showed that the egg stage was the longest during generational development, spanning from September of the current year to April of the subsequent year. The nymph stage persisted for approximately 2–3 months, with Area 4 being the longest (94 days), and Area 3 being the shortest (71 days). The significant difference was primarily due to Area 4 reaching the initial developmental temperature in mid-April. During this period, most night-time temperatures in Area 4 were below the initial developmental temperature; therefore, only daytime conditions were met for temperature accumulation. In contrast, Area 3 started egg incubation with an average temperature of 10–12 °C, enabling it to accumulate more heat. Consequently, less time was required to complete the incubation in Area 3.

Based on the calculated results of the *D. barbipes* developmental period, the habitat factors of the corresponding period were obtained. Among the 31 factors, soil pH, the temperature of the 1st to 3rd nymph instar, soil temperature of the egg stage, and aspect (Fig. S1) did not have a significant effect on the occurrence of *D. barbipes* ($p > 0.05$) and were therefore removed. Fig. 3b shows some important factors that significantly affected *D. barbipes* (p-value < 0.05). The minimum temperature in the egg period (OMinT) in the no-grasshopper occurrence areas was significantly higher than in grasshopper occurrence areas, with an average temperature difference of 7.2 °C. Furthermore, the findings indicated that total precipitation during the spawning period (SP) also significantly influenced the occurrence of grasshoppers. In areas without grasshoppers, the total precipitation was 199.79 mm, whereas in areas with grasshoppers, it was 917.32 mm. Insufficient precipitation during the spawning period hinders vegetation growth, restricting the availability of food sources essential for grasshopper survival. This study also identified FVC in the nymph stage (Nfvc) as a pivotal factor in determining the occurrence of grasshoppers. The average FVC in *D. barbipes* was 0.26, in contrast, the average FVC in non-occurrence areas was only 0.14, indicating an insufficient food supply

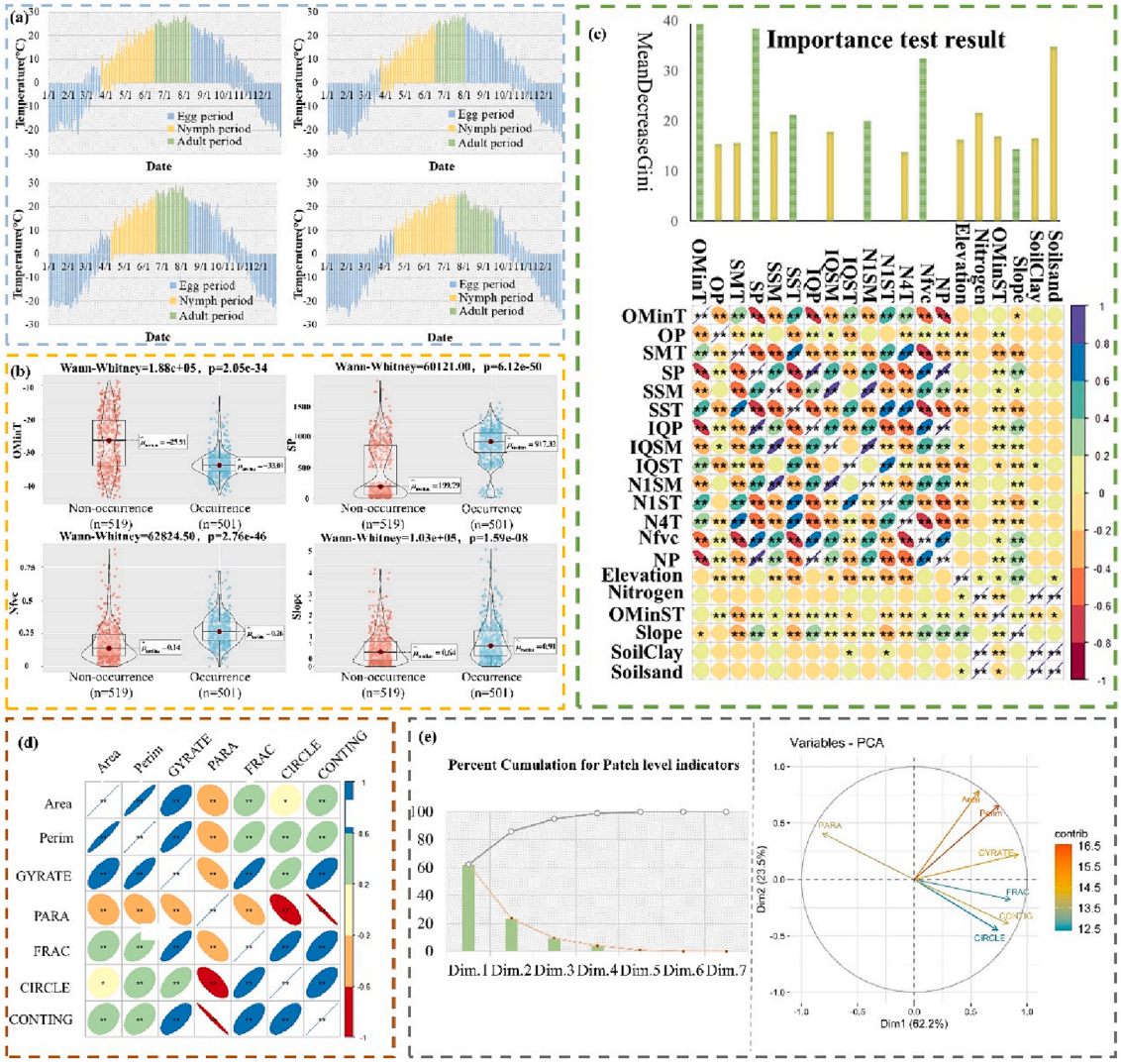


Fig. 3. Results of HDB monitoring indicators construction; (a) Calculation results of the developmental stages of *D. barbipes*; (b) Test results of factors with significant differences; (c) Analysis of local habitat factor correlations and importance test results; (d) Analysis of landscape variable correlations; (e) PCA results of landscape factors.

for grasshoppers to sustain their normal life activities under these conditions. The results also underscored slope as a critical factor influencing grasshopper distribution, with grasshopper occurrence areas exhibiting higher slopes than non-occurrence areas.

After eliminating the factors that showed no significant differences, a correlation analysis was conducted (Fig. 3c). Subsequently, to ensure robust variable selection, the study utilized the random forest algorithm to assess the variable importance, as depicted in Fig. 3c. Factors with correlations > 0.8 and lower importance scores were excluded. SP, OMinT, Nfvc, soil temperature in the spawning period (SST), and soil moisture of the 1st to 3rd nymph instar (N1SM) exhibited high importance scores, and their correlations with other factors were < 0.8; thus, they were retained. However, despite scoring high in the importance test, variables such as soil sand and nitrogen were removed because of their lack of significant correlation with numerous other factors.

Additionally, we conducted a correlation analysis of landscape indicators (Fig. 3d) and employed PCA to select landscape factors. Principal components with a cumulative contribution > 80 % were selected for the analysis (Fig. 3e) (Ghosh-Dastidar et al., 2008). The PCA results revealed that at the patch scale, GYRATE contributed the most to the first principal component, whereas AREA contributed the most to the second. Therefore, these two variables were selected as variables. The GYRATE and AREA are the area and edge index, which means the Radius of Gyration and the area of each patch, respectively. In summary, the monitoring system included eight variables: SP, OMinT, Nfvc, SST, N1SM, Slope, AREA, and GYRATE.

3.2. Spatial pattern characteristics of *D. barbipes*

The spatial autocorrelation results for *D. barbipes* from 2018 to 2023 (Fig. S2) showed that the z-scores fluctuated between 1.74 and 14.28 at a 90 % confidence interval, which were all > 1.65 and had a p-value of < 0.10, suggesting that instead of being random, *D. barbipes* occurrence has a spatial autocorrelation.

Exploring the spatiotemporal dynamics of *D. barbipes* distribution in Xilingol from 2018 to 2023 revealed the following patterns: 1) HAAs were predominantly concentrated in Zheng Lan, XilinHot, West Ujumqin, and East Ujumqin. Notably, XilinHot and West Ujumqin consistently displayed significant aggregation characteristics each year (Fig. 4); 2) the results of aggregation direction and trends (Fig. 5) indicated that the aggregation directions had slight variations each year, but had a consistent trend of aggregation from southwest to northeast in all years; and 3) the centroids of *D. barbipes* were mainly situated in XilinHot and West Ujumqin (Fig. 5). From 2018 to 2021, the centroid continuously

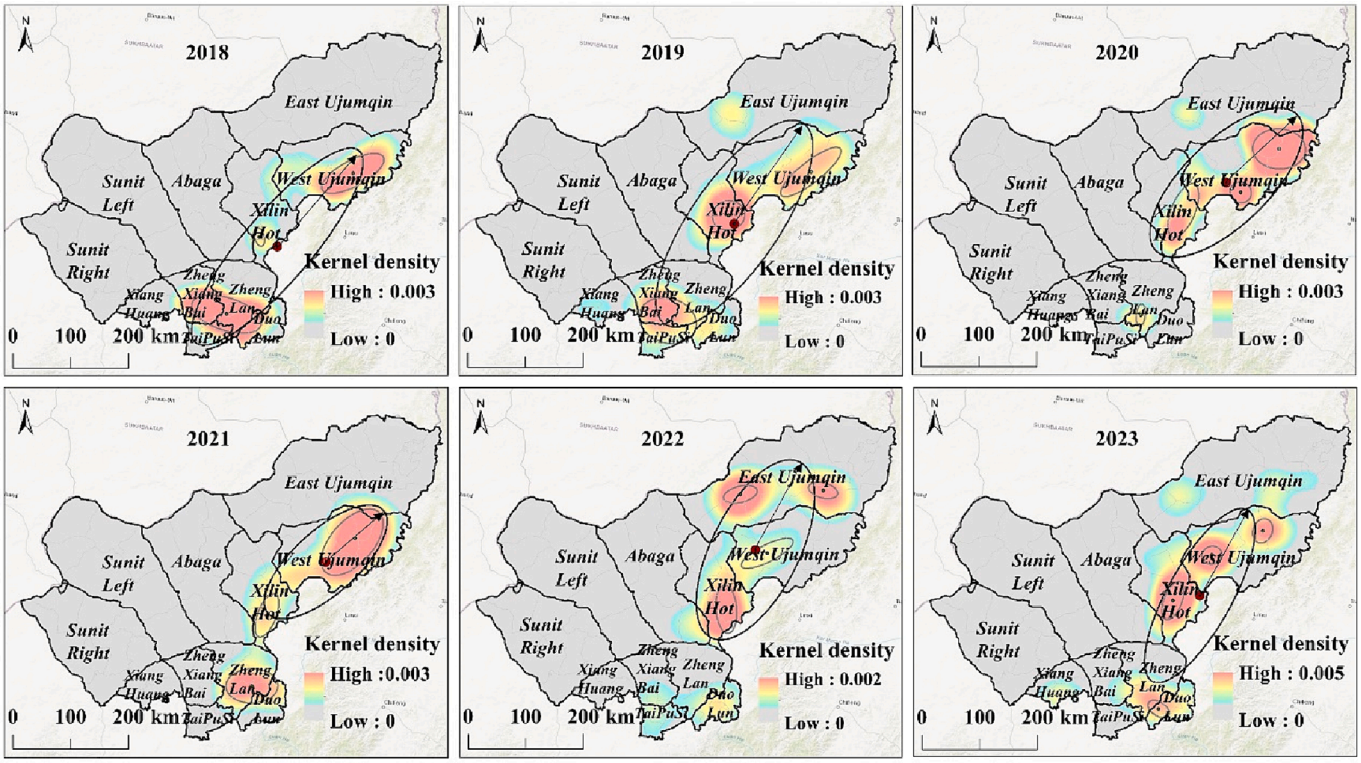


Fig. 4. Spatial distribution characteristics of *D. barbipes*. The red dots represent the centroid of the overall HAA, while the green dots represent the centroids of individual aggregation areas. The black ellipses signify the SDE for each HAA, and the gray ellipses represent the SDE for individual HAAs. (For interpretation of the references to colour in this figure legend, the reader is referred to the web version of this article.)

moved in a northeast direction, shifting northwest in 2021–2022 and southward in 2022–2023.

The spatial distribution patterns for each year were as follows: in 2018, three main HAAs for *D. barbipes* were identified, mainly located in Zheng Lan, Zheng Xiang Bai, XilinHot, and West Ujumqin. The centroid of the occurrences was situated in XilinHot. In 2019, the monitoring results also revealed three HAAs, with longer short axes of the SDE, indicating an east–west expansion of the HAA. The centroid of *D. barbipes* occurrences moved northward (Fig. 5). The HAA in XilinHot expanded further compared with 2018, with the centroid moving northeast and the overall trend changing from southwest to northeast. In 2020, the centroid of the HAA continued its northward movement, reaching West Ujumqin; however, the extent of the HAA was further reduced. Notably, the HAA in XilinHot and West Ujumqin tended to spread northeastward. In 2021, the HAA in XilinHot contracting and the centroid moving southward. Meanwhile, the HAA in west Ujumqin continued to expand and extend toward East Ujumqin. In 2022, the HAA in west Ujumqin contracted, and East Ujumqin showed two HAAs, indicating a suitable environment for grasshopper survival. In 2023, HAAs exhibited an overall northeastern trend and were primarily in ZhengLan, DuoLun, XilinHot, and West Ujumqin. Several HAAs showed increasing trends, highlighting the need for attention.

3.3. Monitoring results of HDB

The monitoring results for the validation of the L-GWLR model (Table 1) indicated that the AIC of the L-GWLR model for each year was consistently lower than that of the other three models. Based on the analysis of D^2, the D^2 of the L-GWLR model was higher than those of the other three models. These results imply that the L-GWLR model, which incorporates landscape and spatial heterogeneity, outperformed the GWLR model, which solely considers spatial heterogeneity, as well as the traditional LR and OLS models, which overlook spatial heterogeneity. Therefore, this model proved to be well-suited for monitoring HDB.

By analyzing the monitoring results of the best-performing model (L-GWLR) and the statistical areas of the three suitability levels in the main counties (Fig. 6), we discovered that the most suitable habitats for *D. barbipes* ranged from 27,357 to 51,736 km^2, occupying 13.48 % to 25.49 % of the total study area. These areas were predominantly concentrated in XilinHot, East Ujumqin, West Ujumqin, Zheng Lan, Xiang Huang, and Duo Lun. Notably, XilinHot, West Ujumqin, East Ujumqin, and Zheng Lan consistently possessed the most suitable habitats throughout the year. Conversely, in Sunit Right, Sunit Left, and Abaga, less suitable habitats predominated in over 95 % of the regions, with a grasshopper occurrence probability < 0.5.

The annual monitoring results indicated that in 2018, East Ujumqin had the largest most suitable habitat area, reaching 14,019 km^2, followed by West Ujumqin, which covered 5,148 km^2. XilinHot and Zheng Lan have areas of 3,632 km^2 and 1,824 km^2, respectively. In 2019, the most suitable habitats for both West and East Ujumqin expanded, reaching 9,467 km^2 and 14,932 km^2, respectively. The spatial distribution showed that the augmented areas were primarily situated in the central and northern of East Ujumqin and the western and eastern parts of West Ujumqin. Furthermore, the most suitable habitats in Xiang Huang and Duo Lun experienced increases of 1,554 km^2 and 883 km^2, respectively, and were concentrated in the central part of Xiang Huang and the northern part of Duo Lun. By 2020, the northern and eastern parts of West Ujumqin mostly transitioned to the most suitable habitats, leading to an increase of 5,403 km^2. The most suitable habitat for XilinHot exceeds 10,000 km^2. Currently, a large portion of the habitats in West Ujumqin and XilinHot are conducive to the survival and reproduction of grasshoppers. Furthermore, the most suitable habitat in East Ujumqin increased by 1,713 km^2, concentrated in the eastern region. Conversely, the occurrence probability of grasshoppers in Xiang Huang, Zheng Xiang Bai, and Duo Lun decreased compared with 2019.

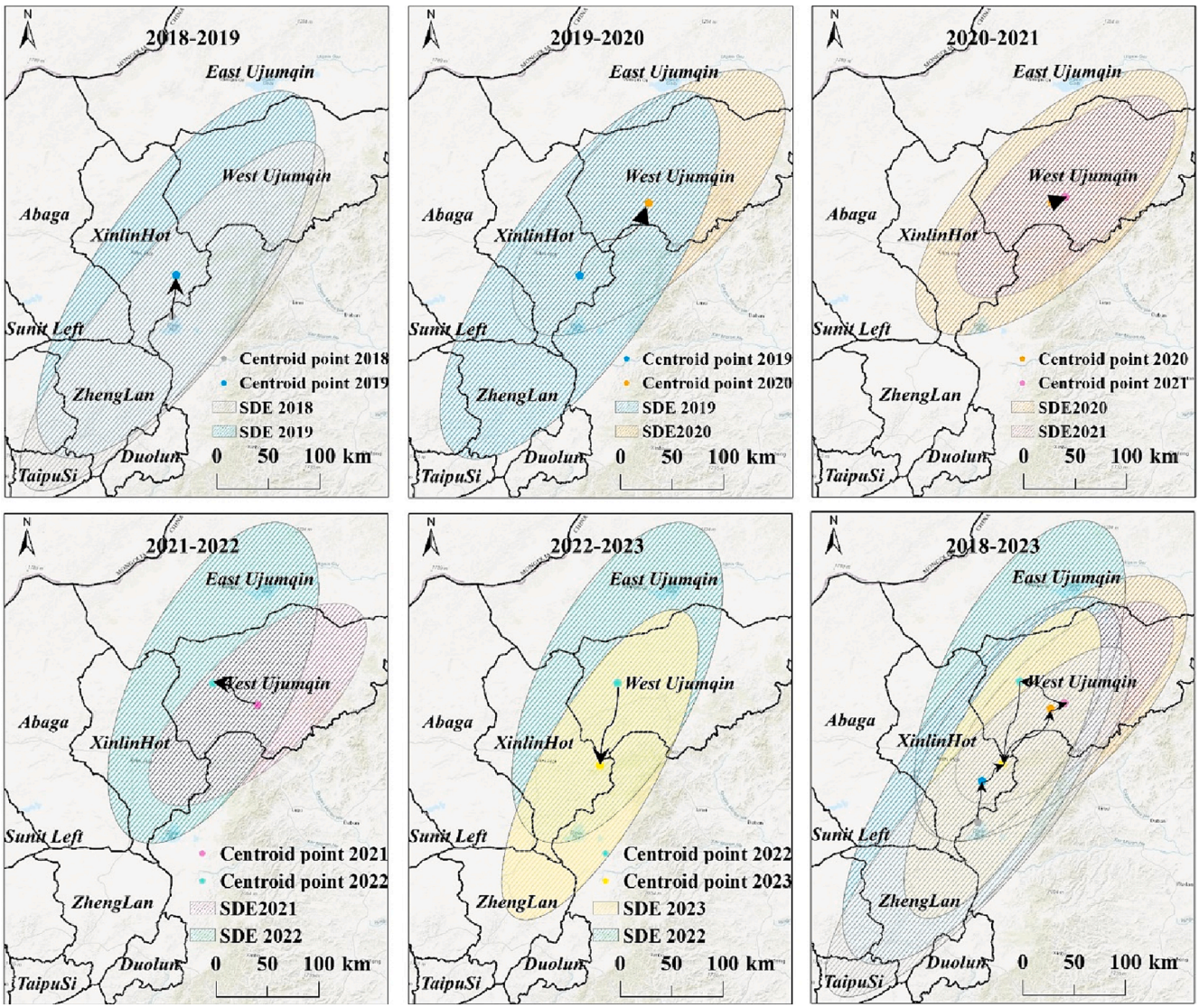


Fig. 5. Migration and changes in centroids and HAAs of *D. barbipes* from 2018 to 2023.

In 2021, the most suitable habitat for XilinHot remained large, at 10,399 km^2. Additionally, the habitat conditions in Zheng Lan, Duo Lun, and TaiPuSi were also suitable, leading to an increase of 3,605 km^2 in the most suitable habitat, especially in the southern part of Zheng Lan, most parts of Duo Lun, and the northeastern part of TaiPuSi. However, the probability of grasshopper occurrence significantly decreased in the eastern and western Ujumqin. Most of East Ujumqin, previously identified as the most suitable habitat, transitioned to a moderately suitable habitat, and the most suitable habitat in the eastern and northern parts of West Ujumqin has shifted to a moderately suitable habitat. In 2022, the most suitable habitat reached its highest level in all years. West Ujumqin has the largest habitat, reaching 20,597 km^2, surpassing all other counties. Only a few areas in the east were unsuitable. In 2022, the eastern of East Ujumqin once more transitioned into the most suitable habitat, resulting in an expansion of 11,969 km^2 in the most suitable habitat. The most suitable habitat in the southern remained concentrated in the southern part of Duo Lun and Zheng Lan. In 2023, the most suitable habitat in the northern and eastern parts of West Ujumqin decreased by 2,801 km^2 because of the transition from the most suitable habitat to a moderately suitable habitat. In contrast, unsuitable habitats in the eastern and northern parts of western Ujumqin shifted to moderately suitable habitats. Compared with that in 2022, the most suitable habitats in the central and northern parts of XilinHot decreased by 5,155 km^2. The most and moderately suitable habitats for Duo Lun and TaiPuSi also decreased.

3.4. Driving indicators for HDB changes

By analyzing the monitoring results of the L-GWLR model, distinctive variations in specific regions from 2018 to 2023 were identified, particularly in East Ujumqin and XilinHot. The changes in HDB were driven by habitat indicators. To investigate the reasons behind these changes, this study adopted pastures as fundamental units and analyzed the indicators driving the changes in major pastures (Fig. 7). The spatial distribution of major pastures is shown in Fig. 2.

In the years 2019–2020 and 2021–2022, a noteworthy transition occurred in the eastern part of East Ujumqin, particularly in the ALaTanHeLi and EjiNaoEr pastures, where most areas became the most suitable habitats. An analysis of the driving indicators for these pastures revealed that in 2020 and 2022, the OMinT in these two pastures ranged from –33 °C to –29 °C, which was higher than in other years. Winter temperatures between −35 °C and −28 °C are favorable for the survival of grasshoppers, as excessively low temperatures can lead to the death of grasshopper eggs (Branson, 2020). Additionally, the Nfvc in these pastures ranged from 0.2 to 0.25, signifying ample vegetation to meet the food source requirements and adequate sunlight for normal life

Table 1
Evaluation of performance among the models.

Year	Method	AIC	D^2
2018	L-GWLR	86.51	0.718
	GWLR	94.184	0.663
	LR	124.68	0.443
	OLS	98.623	0.410
2019	L-GWLR	74.831	0.790
	GWLR	78.769	0.684
	LR	104.308	0.576
	OLS	90.086	0.527
2020	L-GWLR	124.256	0.737
	GWLR	133.719	0.537
	LR	211.04	0.28
	OLS	190.091	0.258
2021	L-GWLR	60.8	0.785
	GWLR	99.785	0.356
	LR	149.065	0.231
	OLS	108.961	0.360
2022	L-GWLR	97.040	0.710
	GWLR	127.755	0.267
	LR	166.585	0.313
	OLS	137.112	0.294
2023	L-GWLR	169.556	0.427
	GWLR	202.252	0.256
	LR	311.823	0.125
	OLS	182.090	0.179

activities. The combined effects of Nfvc and OMinT led to the expansion of suitable habitats for *D. barbipes* in the ALaTanHeLi and EjiNaoEr pastures. In 2019, EjiNaoEr experienced an OMinT of –31.54 °C, similar to the range of –33 °C to –29 °C, but its Nfvc was only 0.16. During the nymph stage, when grasshopper feeding peaks, the insufficient vegetation did not meet the basic food requirements of *D. barbipes*.

From 2020 to 2022, certain pastures in XilinHot, specifically ChaoKeWuLa, BaYanBaoLaGe, and BaoLiGen, consistently had the most suitable habitats, whereas their suitability was comparatively lower in 2018, 2019, and 2023. An examination of the driving indicators for these pastures revealed that during the period from 2020 to 2022, the ChaoKeWuLa pasture had an SP between 800 and 900 mm, Nfvc between 0.2 and 0.26, and SST of 22.8–23.8 °C. Similarly, the BaYanBaoLaGe pasture had an SP between 743 and 911 mm, Nfvc between 0.2 and 0.25, and SST between 22.76 and 24.11 °C. Furthermore, the BaoLiGen pasture had an SP between 724 and 975 mm, Nfvc between 0.2 and 0.22, and SST between 22.36 and 23.50 °C. These findings indicate that during the nymph stage, the suitable FVC, an adequate amount of SP, and suitable SST contributed to the increase of the most suitable habitats in these pastures, making them more suitable for the survival of *D. barbipes*. In 2023, BaoLiGen had an Nfvc ranging from 0.2 to 0.25, but its SP was only 526 mm. Insufficient precipitation during the spawning period not only hinders vegetation growth but also leads to dehydration and mortality of grasshopper eggs. This further emphasizes that the occurrence of grasshoppers is influenced not by a single factor, but by the combined effects of multiple indicators.

The above analysis revealed that the effect of the lowest temperature during the egg period on grasshoppers was primarily evident in East Ujumqin. Situated in a high-latitude region, East Ujumqin experiences cold winters, making the lowest temperatures an important factor. Nfvc has an important influence on both high- and low-latitude regions. In low-latitude regions, the total precipitation during the spawning period and soil temperature play crucial roles.

4. Discussion

The occurrence of grasshoppers is influenced by various factors, including meteorology, soil, vegetation, topography, and ecology. Therefore, identifying representative and irreplaceable monitoring indicators based on numerous habitat factors is crucial. In this study, based on the occurrence and development mechanism of *D. barbipes*, a degree day model was coupled to calculate the growth and development period of *D. barbipes*. Compared with previous studies that empirically divided the growth period of grasshoppers, this method improved the accuracy of growth period division (Du et al., 2022), making the time range of monitoring indicators more precise. Additionally, coupled with difference, correlation, importance, and PCA analyses, eight representative monitoring indicators were selected. In contrast with most studies on grasshopper monitoring that rely on empirically selected monitoring indicators or only consider the correlation between factors, neglecting the importance and differences between factors (Zhang et al., 2023), this study significantly improved the representativeness and indispensability of monitoring indicators.

From a modeling perspective, this study is based on the development mechanism of *D. barbipes*, combined with the landscape and spatial characteristics building the monitoring model. The performance of L-GLWR indicated that the method considering landscape and spatial characteristics outperformed those considering only spatial or landscape characteristics. These results suggest that the occurrence of *D. barbipes* is influenced by a combination of both landscape and spatial characteristics. The model established in this study is comprehensive and contributes to improving the capabilities of monitoring and early warning for grasshoppers.

The analysis of the monitoring results also showed that the HDB of the L-GWLR model result was larger than that of the HAAs result based on point analysis, especially in East Ujumqin, which highlights the limitations of point-based investigations. Continuous spatiotemporal data from multiple sources provides an intuitive understanding of the spatiotemporal distribution of HDB, compensating for the shortcomings of point-based monitoring methods.

However, some shortcomings recognized, and future research should address the following aspects: 1) the study only covers the years 2018–2023; hence, subsequent research should include the analysis of longer time series data to enhance the monitoring capabilities of the model; 2) the analysis in this study was based on the occurrence and non-occurrence points of *D. barbipes*. Future research should consider the severity of *D. barbipes* infections to better understand the extent of infestation; 3) This study mainly focused on Xilingol, a city in Inner Mongolia. While Xilingol was the primary area of interest due to its relevance to the grasshopper issue, it's worth noting that many regions are affected by grasshoppers. Therefore, in future research, the methods of this study can extend to other regions as well; 4) This study focuses on analyzing *D. barbipes*, due to its most widespread, numerous, and densely populated. The research methodology utilized in this study is based on the occurrence of both grasshopper occurrence and non-occurrence points, without being confined by species specificity. Thus, in forthcoming studies, there exists the prospect to broaden this methodology to encompass the monitoring and analysis of suitable habitats for various other grasshopper species, as well as to extend its application to the surveillance of habitats conducive to other pest species.

5. Conclusion

This study established representative monitoring indicators for *D. barbipes* and conducted a spatiotemporal pattern analysis of *D. barbipes* occurrence from 2018 to 2023 to investigate their spatial characteristics and HAAs. Moreover, the L-GWLR was constructed by integrating meteorological, vegetation, soil, topographic, and ecological data from multiple sources while considering landscape and spatial heterogeneity. Subsequently, the model was applied to monitor HDB from 2018 to 2023, accompanied by an analysis of the driving factors of its changes. The results indicated that the distribution of *D. barbipes* had significant spatial autocorrelation, and several HAAs were observed. Furthermore, the performance of the L-GWLR model surpassed that of the monitoring models that neglected landscape or spatial characteristics, demonstrating its applicability for monitoring the HDB of *D. barbipes*. The analysis of the monitoring results revealed that HDB was

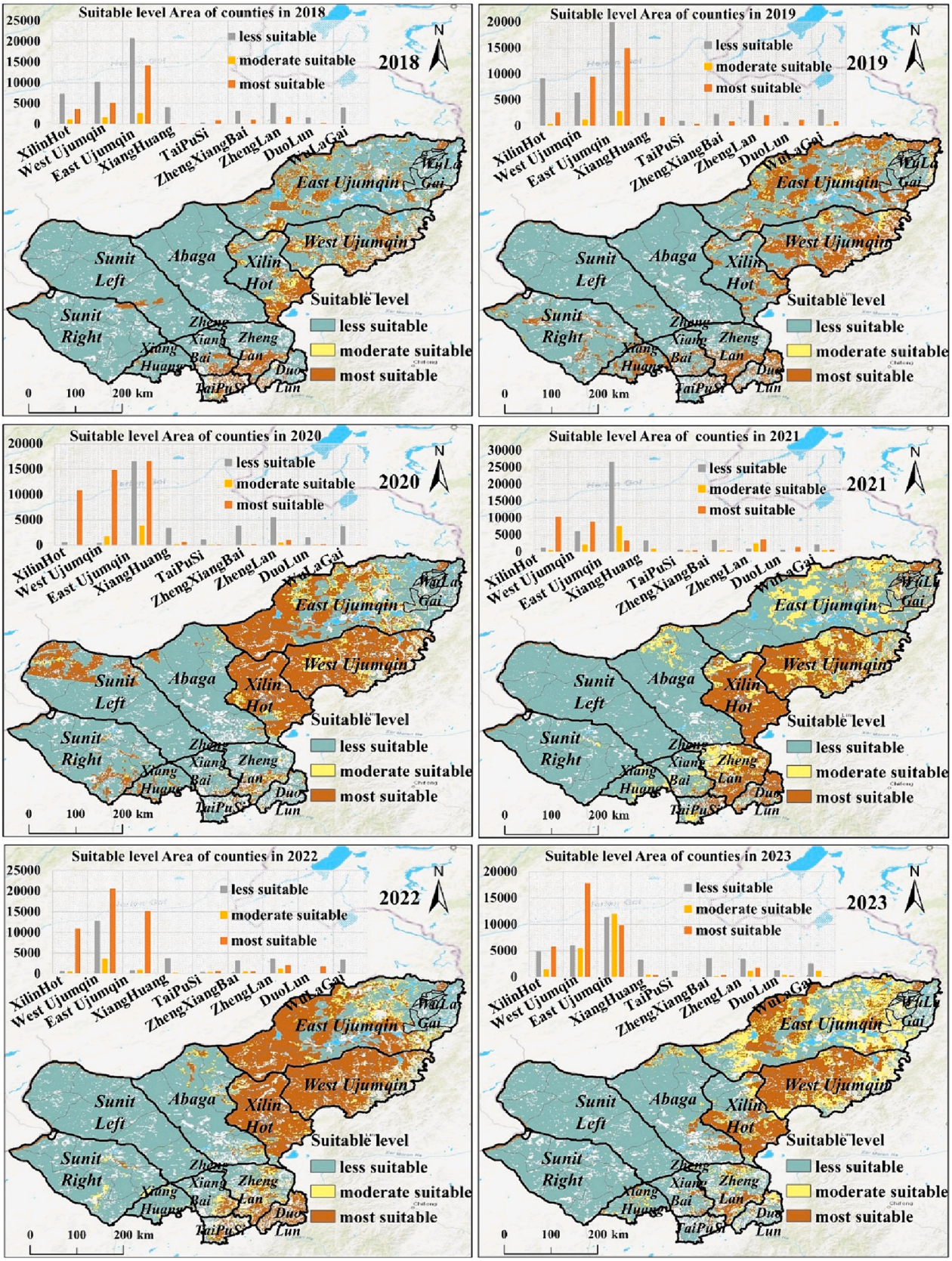


Fig. 6. Monitoring results of the L-GWLR model and the areas of each suitability level in the main counties.

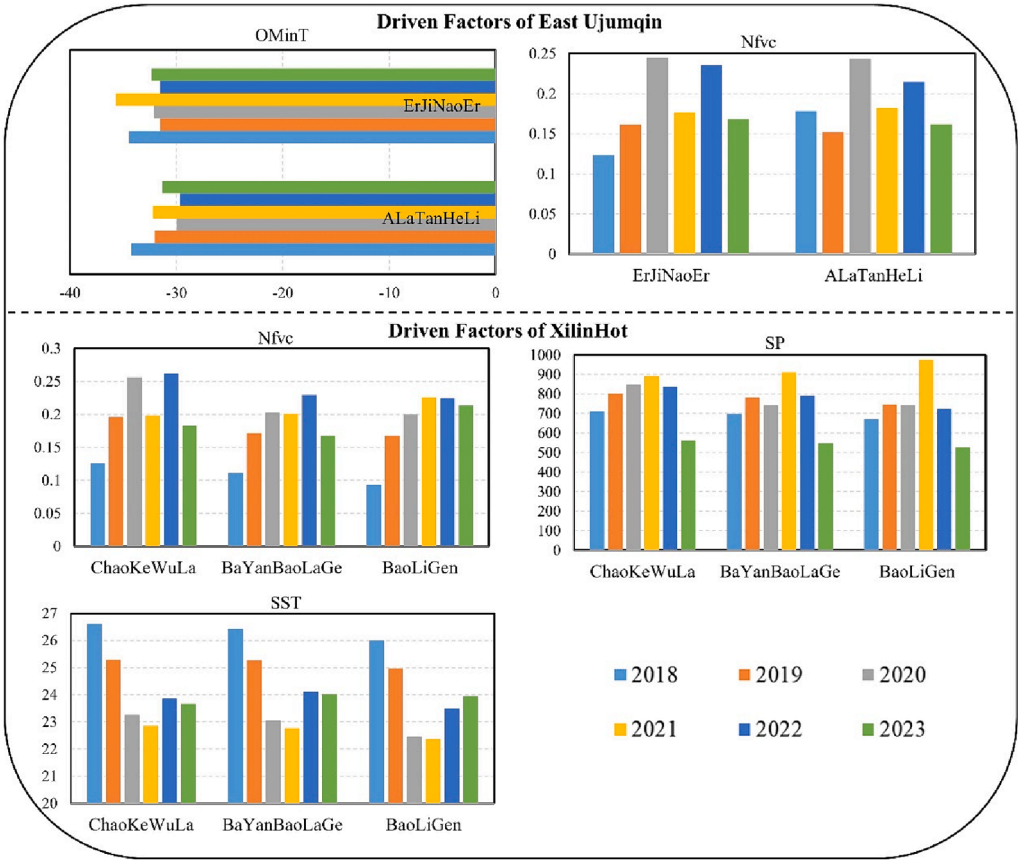


Fig. 7. Driving indicators of the HDB suitability in major pastures.

primarily concentrated in XilinHot, West Ujumqin, East Ujumqin, and Zheng Lan. The spatial extent of the HDB monitoring results larger range of HAAs based on point analysis, indicating that the use of continuous spatiotemporal data compensated for the incompleteness of point-based monitoring. The findings presented herein provide a basis for the precise prevention and control of grasshoppers. Plant protection departments should pay more attention to the grasshopper population and density in the most suitable and moderate areas and take timely preventive and control measures. These findings can also guide the plant protection departments to develop the survey routes.

Funding

This work was supported by National Key R & D Program of China (2022YFD1401102), project of Northern Agriculture and Livestock Husbandry Technical Innovation Center, Chinese Academy of Agricultural Sciences (BFGJ2022002), Fengyun Application Pioneering Project (FY-APP).

CRediT authorship contribution statement

Jing Guo: Writing – review & editing, Writing – original draft, Visualization, Formal analysis, Data curation. **Wenjiang Huang:** Writing – review & editing, Funding acquisition. **Yingying Dong:** Writing – review & editing, Methodology, Conceptualization. **Kejian Lin:** Resources, Project administration. **Yantao Zhou:** Writing – review & editing, Visualization. **Ning Wang:** Resources, Project administration. **Rui Hua:** Writing – review & editing, Validation. **Zhuoqing Hao:** Supervision, Software. **Xiaolong Ding:** Data curation, Investigation. **Fei Zhao:** Supervision, Validation.

Declaration of competing interest

The authors declare that they have no known competing financial interests or personal relationships that could have appeared to influence the work reported in this paper.

Data availability

The authors do not have permission to share data.

Acknowledgments

The authors would like to sincerely thank Yanru Huang, and Mingxian Zhao for their help with the study. We also thank the academic editors and reviewers for their insightful comments which greatly helped us improve the quality of this manuscript

Appendix A. Supplementary data

Supplementary data to this article can be found online at https://doi.org/10.1016/j.jag.2024.103838.

References

Ahmad, M.N., Shao, Z., Altan, O., 2022. Effect of locust invasion and mitigation using remote sensing techniques: a case study of North Sindh Pakistan. Photogramm. Eng. Remote Sens. 88, 47–53. https://doi.org/10.14358/pers.21-00025r2.

Bernard, B., Watsusi, C.W., Gudoyi, P.M., Lutaaya, N., Gumisiriza, L.T., Magaya, J.P., 2023. Desert locust invasion in uganda: effects on household food consumption and effective control interventions. Sustainability 15, 14496. https://doi.org/10.3390/su151914496.

Branson, D.H., 2020. Influence of cold temperature and exposure time on egg overwintering survival in the white-whiskered grasshopper (Orthoptera: Acrididae). J. Orthoptera Res. 29, 63–65. https://doi.org/10.3897/jor.29.46967.

Chen, G., 2008. Effects of temperature and photoperiod on the growth, development and egg diapause of three grasshopper species in Inner Mongolia. (Master's), Inner Mongolia Agricultural University, Inner Mongolia (In Chinese).
Coxwell, C.C., Bock, C.E., 1995. Spatial variation in diurnal surface temperatures and the distribution and abundance of an alpine grasshopper. Oecologia 104, 433–439.
Dong, Z., Zhang, J., Tong, Z., Han, A., Zhi, F., 2022. Ecological security assessment of Xilingol grassland in China using DPSIRM model. Ecol. Indic. 143 https://doi.org/10.1016/j.ecolind.2022.109336.
Du, B., Wei, J., Lin, K., Lu, L., Ding, X., Ye, H., Huang, W., Wang, N., 2022. Spatial and Temporal Variability of Grassland Grasshopper Habitat Suitability and Its Main Influencing Factors. Remote Sens. 14, 3910. https://doi.org/10.3390/rs14163910.
Edwards, R.L., Epp, H.P., 1965. The Influence of Soil Moisture and Soil Type on the Oviposition Behaviour of the Migratory Grasshopper, Melanoplus sanguinipes (Fahricius). Can. Entomol. 97, 401–409. https://doi.org/10.4039/Ent97401-4.
Gauffre, B., Mallez, S., Chapuis, M.P., Leblois, R., Litrico, I., Delaunay, S., Badenhausser, I., 2015. Spatial heterogeneity in landscape structure influences dispersal and genetic structure: empirical evidence from a grasshopper in an agricultural landscape. Mol. Ecol. 24, 1713–1728. https://doi.org/10.1111/mec.13152.
Ge, Y., Shen, H., Liu, J., 2009. Impacts of climate change on historical locust outbreaks in China. J. Geophys. Res. Atmos. 114, D18104. https://doi.org/10.1029/2009jd011833.
Geng, Y., Zhao, L., Dong, Y., Huang, W., Shi, Y., Ren, Y., Ren, B., 2020. Migratory Locust Habitat Analysis With PB-AHP Model Using Time-Series Satellite Images. IEEE Access 8, 166813–166823. https://doi.org/10.1109/access.2020.3023264.
Getis, A., Ord, J.K., 1992. The analysis of spatial association by use of distance statistics. Geographical analysis 24 (3), 189–206.
Ghosh-Dastidar, S., Adeli, H., Dadmehr, N., 2008. Principal component analysis-enhanced cosine radial basis function neural network for robust epilepsy and seizure detection. IEEE Trans. Biomed. Eng. 2, 512–518. https://doi.org/10.1109/TBME.2007.905490.
Gómez, D., Salvador, P., Sanz, J., Casanova, C., Taratiel, D., Casanova, J.L., 2019. Desert locust detection using Earth observation satellite data in Mauritania. J. Arid Environ. 164, 29–37. https://doi.org/10.1016/j.jaridenv.2019.02.005.
Gómez, D., Salvador, P., Sanz, J., Casanova, J.L., 2020. Modelling desert locust presences using 32-year soil moisture data on a large-scale. Ecol. Indic. 117 https://doi.org/10.1016/j.ecolind.2020.106655.
Guo, J., Zhao, L., Huang, W., Dong, Y., Geng, Y., 2022. Study on the Forming Mechanism of the High-Density Spot of Locust Coupled with Habitat Dynamic Changes and Meteorological Conditions Based on Time-Series Remote Sensing Images. Agronomy 12, 1610. https://doi.org/10.3390/agronomy12071610.
Guo, J., Lu, L., Dong, Y., Huang, W., Zhang, B., Du, B., Ding, C., Ye, H., Wang, K., Huang, Y., Hao, Z., Zhao, M., Wang, N., 2023. Spatiotemporal Distribution and Main Influencing Factors of Grasshopper Potential Habitats in Two Steppe Types of Inner Mongolia, China. Remote Sens. 15, 866. https://doi.org/10.3390/rs15030866.
Guo, Y., 2007. The occurrence and control strategies of grasshoppers in the grasslands of Xilingol League, Inner Mongolia. Inner Mongolia Prataculture, 19, 30-33. Doi:1009-1866(2007)03-0030-04 (In Chinese).
Huang, J., Bai, Y., Jiang, Y., 2009. Case study 3: Xilingol grassland, Inner Mongolia. In: Rangeland Degradation and Recovery in China's Pastoral Lands. CABI, Wallingford UK, pp. 120–135.
Humphreys, J.M., Srygley, R.B., Branson, D.H., 2022. Geographic variation in migratory grasshopper recruitment under projected climate change. Geographies 1, 12–30. https://doi.org/10.3390/geographies2010003.
Klein, I., Uereyen, S., Eisfelder, C., Pankov, V., Oppelt, N., Kuenzer, C., 2023. Application of geospatial and remote sensing data to support locust management. Int. J. Appl. Earth Obs. Geoinf. 117, 103212 https://doi.org/10.1016/j.jag.2023.103212.
Latchininsky, A.V., 2008. Grasshopper outbreak challenges conservation status of a small Hawaiian Island. J. Insect Conserv. 12 (3–4), 343–357.
Li, H., Zhang, Y., Wang, G., Lowry, A., Huang, W., Dong, Y., Shang, S., Luke, B., 2021. The Effects of Vegetation Type on Oedaleus decorus asiaticus (Orthoptera: Acrididae) Oviposition and Hatching Success. Environ. Entomol. 50, 790–794. https://doi.org/10.1093/ee/nvab029.
Lian, Y., Leng, J., 2007. Discussion on Grassland Ecological Construction and Protection in Xilingol League. Rural Financ. 12, 23. In Chinese.
Liu, L., 2020. Study on The Optimization of Ecological Management of Xilinguole Grassland. (Master's), Fujian Normal University, Fujian.
Löw, F., Waldner, F., Latchininsky, A., Biradar, C., Bolkart, M., Colditz, R.R., 2016. Timely monitoring of Asian Migratory locust habitats in the Amudarya delta, Uzbekistan using time series of satellite remote sensing vegetation index. J. Environ. Manage. 183, 562–575. https://doi.org/10.1016/j.jenvman.2016.09.001.
Meynard, C.N., Lecoq, M., Chapuis, M.P., Piou, C., 2020. On the relative role of climate change and management in the current desert locust outbreak in East Africa. Glob. Change Biol. 26, 3753–3755. https://doi.org/10.1111/gcb.15137.
O'Mara, F.P., 2012. The role of grasslands in food security and climate change. Annals of botany 110 (6), 1263–1270.
Pegel, U., Pfeiffer, K., Zittrell, F., Scholtyssek, C., Homberg, U., 2019. Two Compasses in the Central Complex of the Locust Brain. J. Neurosci. 39, 3070–3080. https://doi.org/10.1523/JNEUROSCI.0940-18.2019.
Petermann, J.S., Buzhdygan, O.Y., 2021. Grassland biodiversity. Curr. Biol. 31, R1195–R1201. https://doi.org/10.1016/j.cub.2021.06.060.
Piou, C., Lebourgeois, V., Benahi, A.S., Bonnal, V., Jaavar, M.E.H., Lecoq, M., Vassal, J.-M., 2013. Coupling historical prospection data and a remotely-sensed vegetation index for the preventative control of Desert locusts. Basic Appl. Ecol. 14, 593–604. https://doi.org/10.1016/j.baae.2013.08.007.
Qiu, X., Kang, L., Li, H.C., 2004. The economic threshold for control of the major species of grasshoppers on Inner Mongolian rangeland. Acta Entomol. Sin. 5, 595–598. https://doi.org/10.16380/j.kcxb.2004.05.009 (In Chinese).
Shen, J., Zhang, N., He, B., Liu, C.Y., Li, Y., Zhang, H.Y., Chen, X.Y., Lin, H., 2015. Construction of a GeogDetector-based model system to indicate the potential occurrence of grasshoppers in Inner Mongolia steppe habitats. Bull. Entomol. Res. 105, 335–346. https://doi.org/10.1017/S0007485315000152.
Shi, Y., Huang, W., Dong, Y., Peng, D., Zheng, Q., Yang, P., 2018. The influence of landscape's dynamics on the Oriental Migratory Locust habitat change based on the time-series satellite data. Journal of environmental management 218, 280–290.
Sivakumar, M,V.K., Lal, R., Selvaraju, R., Hamdan, I. (Eds.), 2013. Climate Change and Food Security in West Asia and North Africa. Springer, Dordrecht.
Steck, C.E., Bürgi, M., Coch, T., Duelli, P., 2006. Hotspots and richness pattern of grasshopper species in cultural landscapes. Biodivers. Conserv. 16, 2075–2086. https://doi.org/10.1007/s10531-006-9089-7.
Tappan, G.G., Moore, D.G., Knausenberger, W.I., 1991. Monitoring grasshopper and locust habitats in Sahelian Africa using GIS and remote sensing technology. Int. J. Geogr. Inf. Syst. 5, 123–135. https://doi.org/10.1080/02693799108927836.
Tu, X., Du. G., Li, C., Wei, Y., Zhang, W., Yuan, X., Hong, J., Li, Y., Wang, B., Zhao, L., Zhang, R., Pang, B., Duan, T., Liu, Y., Liu, C., Liu, X., Li, Z., Yang, D., Cong, B., Ji, M., Wang, X., Wang, G., Zhang, Z., Nan, Z., 2015. Research Progress in Biological Control of Rangeland Pests in China. Chin. J. Biol. Control, 5, 780-788 (In Chinese). doi:10.16409/j.cnki.2095-039x.2015.05.018.
Vennard, C., Nguama, B., Dillion, H.J., Oouchi, H., Chanhley, A.K., 1998. Effects of the Juvenile Hormone Mimic Pyriproxyfen on Egg Development, Embryogenesis, Larval Development, and Metamorphosis in the Desert Locust Schistocerca gregaria (Orthoptera: Acrididae). Ecotoxicology 1, 41–49. https://doi.org/10.1093/jee/91.1.41.
Wachter, D.H., O'Neill, K.M., Kemp, W.P., 1998. Grasshopper (Orthoptera: Acrididae) communities on an elevational gradient in southwestern Montana. J. Kans. Entomol. Soc. 71, 35–43.
Waldner, F., Ebbe, M., Cressman, K., Defourny, P., 2015. Operational Monitoring of the Desert Locust Habitat with Earth Observation: An Assessment. ISPRS Int. J. Geoinf. 4, 2379–2400. https://doi.org/10.3390/ijgi4042379.
Xu, R., Yang, Z.-H., Wang, Q.-P., Bai, Y., Liu, J.-B., Zheng, Y., Zhang, Y.-R., Xiong, W.-P., Ahmad, K., Fan, C.-Z., 2018. Rapid startup of thermophilic anaerobic digester to remove tetracycline and sulfonamides resistance genes from sewage sludge. Sci. Total Environ. 612, 788–798. https://doi.org/10.1016/j.scitotenv.2017.08.295.
Zhang, X., Huang, W., Ye, H., Lu, L., 2023. Study on the Identification of Habitat Suitability Areas for the Dominant Locust Species Dasyhippus Barbipes in Inner Mongolia. Remote Sens. 15, 1718. https://doi.org/10.3390/rs15061718.
Zhang, L., Lecoq, M., Latchininsky, A., Hunter, D., 2019. Locust and Grasshopper Management. Annu. Rev. Entomol. 64, 15–34. https://doi.org/10.1146/annurev-ento-011118-112500.
Zhao, L., Huang, W., Chen, J., Dong, Y., Ren, B., Geng, Y., 2020. Land use/cover changes in the Oriental migratory locust area of China: Implications for ecological control and monitoring of locust area. Agric. Ecosyst. Environ. 303, 107110 https://doi.org/10.1016/j.agee.2020.107110.